# OPTIMIZATION OF RNAV NOISE ABATEMENT ARRIVAL TRAJECTORIES

**R.H. Hogenhuis*, S.J. Hebly**, H.G.Visser***
***Delft University of Technology, Delft, The Netherlands**
**** National Aerospace Laboratory, Amsterdam, The Netherlands**

**Keywords**: *trajectory optimization, noise abatement, RNAV procedures*

## Abstract

*This paper describes the development of a novel tool for the design of environmentally optimized Area Navigation (RNAV) approach procedures. This new development is an extension of a tool called NOISHHH which was developed earlier for the analysis and design of noise abatement procedures around airports. The NOISHHH tool is essentially a framework that combines a noise model, a Geographic Information System, an emissions inventory model and a dynamic trajectory optimization algorithm to generate flight paths that minimize the noise impact in the vicinity of an airport, while satisfying all operational and safety constraints. The RNAV-extended version of NOISHHH offers the possibility to calculate routes that can be programmed into the Flight Management System (FMS) currently available in most aircraft cockpits. The capabilities of the RNAV-compatible version of NOISHHH are illustrated in an example scenario based on an instrument approach to one of the runways of Schiphol airport in the Netherlands.*

## 1 Introduction

The noise resulting from flight operations at major airports is a continuing source of annoyance in nearby residential communities. To mitigate the impact of aircraft noise, a range of strategic and operational measures has been implemented at airports located close to sensitive communities [1]. One option to reduce the noise impact is to re-shape the arrival and departure trajectories into and out of an airport. For this purpose, noise-abatement routes and procedures have been designed and implemented. To date, a number of different noise abatement procedures are in use. In The Netherlands, for example, noise abatement procedures are applied during the night time for approaches to Amsterdam Airport Schiphol [2]. The applied procedures, enabled by modern guidance and navigation technology such as Area Navigation (RNAV) and Flight Management System (FMS), allow aircraft to descend continuously from high altitude without any level flight segment at low altitude. The higher flight path of the Continuous Descent Approach (CDA) combined with lower engine thrust helps to reduce noise exposure in the communities surrounding the airport. Further noise abatement benefits can be expected when more sophisticated glide slope approaches are permitted, such as the three-degree decelerating approach [3].

With respect to lateral flight path management, RNAV navigation provides several benefits. RNAV was specifically developed to provide more lateral freedom, allowing to make a more complete use of available airspace. The improved navigation accuracy offered by RNAV enables flight tracks to be flown with high precision, allowing track deviations to be kept small. The large flexibility in defining RNAV approaches together with the reduced flight track dispersion allow to shape the approach routes such that overflying the most noise sensitive areas can be avoided.

In [4] a framework is presented for generating RNAV trajectories that minimize noise nuisance, based on the use of a global optimization tool. The numerical results presented in [4] remain restricted to fuel-optimized trajectories though.

In [5-8] a sophisticated tool for the design of flexible-geometry noise abatement procedures, called NOISHHH, is presented. The NOISHHH tool facilitates the development of advanced approach procedures that maximize environmental benefits based on an integrated assessment of multiple relevant factors, including noise, fuel burn, emissions and transit time. To accomplish this, NOISHHH combines a noise model, a noise dose-response relationship, an emission inventory model, a geographic information system, and a dynamic trajectory optimization algorithm.

Although the noise-optimized trajectories produced by the basic NOISHHH tool reveal a huge potential for noise impact reduction, they do not readily lend themselves for direct application to terminal area routing. Indeed, the noise-optimized trajectories obtained using the original NOISHHH tool are rather complex in nature, in the sense that they exhibit fairly extensive lateral maneuvering, multiple speed changes, as well as significant variations in the descent rate or climb rate throughout the trajectory. The fact that the FMS can not navigate the aircraft along these routes represents one of the major drawbacks of the optimized routes produced by NOISHHH. For this reason we set out to modify NOISHHH so that it can calculate routes suitable for RNAV.

Before presenting the RNAV-enhanced version of NOISHHH in Section 3, the original NOISHHH tool is outlined in Section 2. Numerical results are presented in Section 4, and conclusions are drawn in Section 5.

## 2 NOISHHH Optimization Framework

The NOISHHH tool concept has been principally based upon a multi-objective optimization framework [5-8]. The NOISHHH tool features a variety of environmental performance criteria, including, gaseous emissions, fuel burn, and noise exposure. Typically, these different criteria are not compatible; the decision variables that optimize one objective may be far from optimal for the others. Improvement with respect to one particular criterion is often achieved at the expense of one or more of the other environmental criteria. To permit a trade-off, NOISHHH considers a "composite" performance index that essentially consists of a weighted combination of the various environmental criteria.

The emissions inventory implemented in NOISHHH is based on the ICAO Engine Exhaust Emissions Data Bank [9]. At present, the emissions inventory model comprises three pollutants, viz. nitrogen oxides ($NO_x$), carbon monoxide (CO), and unburned hydrocarbons (HC). Moreover, there are several pollutants that are directly proportional to fuel burn, including sulphur oxides ($SO_x$). The local emission performance criteria implemented in NOISHHH correspond to the mass of each of these pollutants emitted below 3,000 ft AGL. Aircraft emissions above that altitude are considered to have no discernable effect at ground level near the airport. Global emission assessment is outside the scope of NOISHHH.

The NOISHHH trajectory-synthesis tool features a range of noise performance criteria. Some of these noise criteria are generic in nature, e.g., a criterion that is based on the total area enclosed within a specified noise level contour, while others are site-specific in the sense that they depend on the density and distribution of the population in the vicinity of a particular airport. A typical example of a site-specific noise criterion is the population count within a specified noise level contour. In the numerical examples presented herein, the noise impact assessment remains restricted to the site-specific criterion *Awakenings*, which represents the number of people within the exposed community that is expected to awake due to a single-event nighttime flyover.

To provide a clear illustration of the trajectory optimization capability of NOISHHH, the numerical examples of the (nighttime) noise abatement trajectories presented in this study are based on a composite performance index that comprises a weighted combination of three

criteria, viz., fuel-consumed *Fuel*, transit time $t_f$ and *Awakenings*:

$$J = k_1 \cdot Fuel + k_2 \cdot t_f + k_3 \cdot Awakenings\,, \qquad (1)$$

where the parameters $K_i$ ($i$ =1,2,3) are the user-selected weighting factors in the composite performance index.

To determine the expected number of awakenings, NOISHHH uses the dose-response relationship as proposed by the Federal Interagency Committee on Aviation Noise (FICAN) [10]. Figure 1 summarizes the results of the experimental study reported in [10], in which aircraft noise was measured in people's bedrooms, while their "behavioral awakening" was simultaneously monitored. The curve shown in Figure 1 specifies the dose-response relationship, which essentially represents a worst-case bound on the percentage of people likely to awake *(%Awakening*) due to a single flyover. The indoor sound level at a particular location is obtained by lowering the outdoor sound level computed for that location by 20.5 dB(A), a value that represents the average transmission loss for a typical home. The methodology for calculating the outdoor noise exposure from each individual aircraft flyover that has been adopted in NOISHHH is based on the well-known Integrated Noise Model (INM) [11]. Combining the indoor SEL with the actual population density distribution gives the number of people likely to awake due to a single flyover.

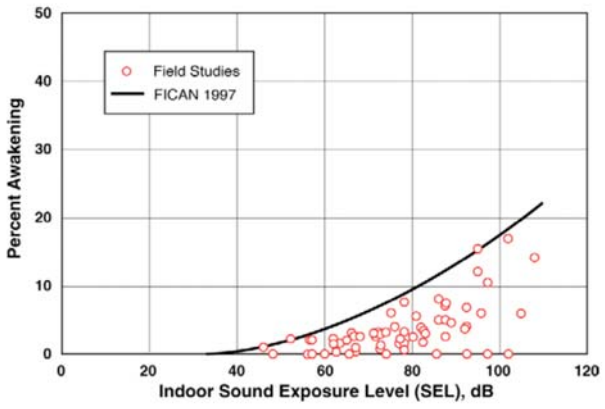


Fig. 1. FICAN proposed sleep disturbance dose-response relationship [10].

To model the movement of an aircraft in three-dimensional (3D) space, INM describes a flight path as a sequence of straight-line segments of finite length. To compute the sound exposure level at a given observer point, the contribution of each segment of the flight-path to the overall result has to be taken into account. The INM procedure for determining the sound exposure level, at any specific observer location, is to select appropriate sound levels from a Noise-Thrust-Distance (NTD) table corresponding to the distances from aircraft to observer. The NTD data contained in the INM database represent the noise exposure levels for specific reference conditions for each aircraft type. To allow for differences between the actual conditions and the reference conditions specified for the NTD tables, a number of noise level adjustments need to be made. Three of those adjustments have been implemented in the current NOISHHH tool, viz., a noise fraction adjustment, a speed adjustment and a lateral attenuation adjustment. Further details can be found in [5-8].

To date, the aircraft characteristics pertaining to three different aircraft types have been implemented in the NOISHHH tool, viz. the Fokker F100 (regional jet), the Boeing 737-300 (narrow body), and the Boeing 747-400 (wide body). In the present study, performance data related to a Boeing 737-300 aircraft have been used. The employed data sets comprise separate drag polars for each flap setting. Also performance data sets are available for aircraft configurations with undercarriage extended.

The INM methodology for sound exposure level computations relies on observer locations that are arranged in the form of a rectangular grid of points surrounding the residential areas in the vicinity of the approach path. The size and mesh of the grid have a significant impact on the computational burden of the iterative optimization process and must therefore be judiciously chosen for each specific case. The numerical examples presented in this paper are based on a scenario which involves an approach from the North-West to runway 18R of Schiphol airport in the Netherlands. Figure 2 illustrates the approach scenario. To be able to

capture the noise impact for the residents immediately surrounding the airport or underneath a flight path, a rectangular grid of fairly large size (50×40 km$^2$) was adopted. To keep the computational burden in check, a relatively large cell size (1×1 km$^2$) was employed. As illustrated in Figure 2, the grid adopted for the noise calculations is also used to define the population distribution.

Figure 2 shows two trajectories, one optimized with respect to fuel consumption and the other with respect to expected awakenings. Both trajectories start at an altitude of 4,000 ft and terminate at 500 ft AGL. Inspection of Figure 2 shows that the fuel-optimized solution starts with a straight line track followed by a turn to provide lateral alignment (ILS localizer) with runway 18R. In contrast, the awakenings-optimized route circumnavigates densely populated areas, before intercepting the localizer. In the noise-optimized solution, the expected number of awakenings decreases by as much as 49 % relative to the minimum-fuel case.

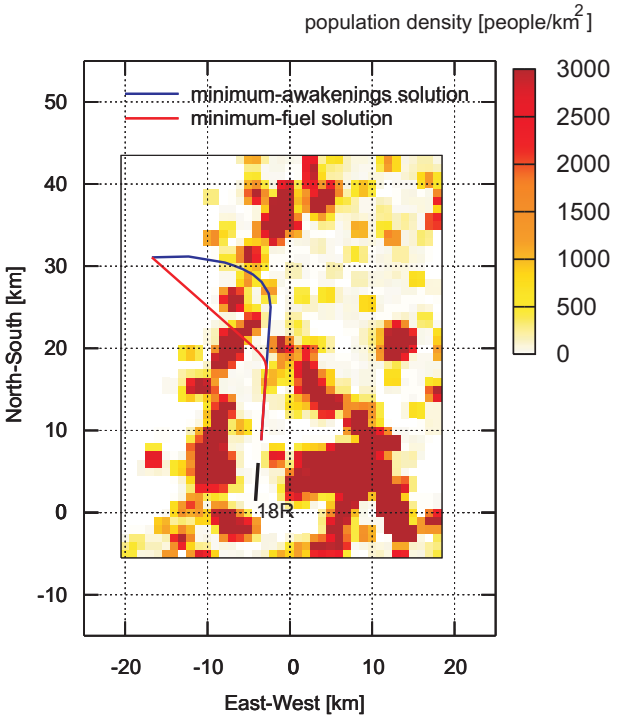


Fig. 2. Comparison between noise and fuel optimized approach trajectories, with underlying noise/population grid area shown.

## 3 RNAV-Compatible Version of NOISHHH

An RNAV procedure can be loosely defined as a sequence of lateral, vertical and speed directives along a set of waypoints, enabling to construct a flight path between waypoints that can be pre-programmed and automatically executed using the FMS technology currently available in most cockpits. In addition to speed and altitude constraints, also time-constraints can be imposed at the waypoints, so that essentially a 4D trajectory solution is obtained. Using RNAV navigation, the aircraft will determine its position using one or more navigation aids such as Distance Measuring Equipment (DME) or Global Navigation Satellite System (GNSS) [12].

An RNAV approach route (horizontal flight path) is built from one or more segments. Each RNAV route segment contains two basic elements, (i) a waypoint, which is a specific location defined by latitude and longitude coordinates, and (ii) a leg type, which defines the path before, after or between waypoints. For RNAV operations a total of 23 different leg types are available. However, for the design of flight routes only two basic leg types are used in NOISHHH, viz., Track-to-Fix (TF) and Radius-to-Fix (RF). A TF leg simply connects two waypoints by a straight line. An RF leg defines a constant radius turn between two waypoints with a fixed radius around a given center point. The RF segment connects two waypoints with a curved path that is tangent to adjoining TF segments.

The vertical flight path is constructed by connecting the speed and altitude constrained waypoints along the horizontal flight path defined by the RNAV route. The vertical navigation mode (VNAV) of the FMS allows building a vertical path between waypoints in several ways. One of the possible vertical navigation modes guides the aircraft from waypoint to waypoint with a constant flight path angle. Due to its generic nature, this particular geometric approach of constructing a point-to-point vertical path has been selected as the basis for the development of the RNAV-compatible version of NOISHHH.

Additional new features implemented in NOISHHH include the possibility to specify constant indicated air speed (IAS) segments, constant deceleration segments, and constant vertical speed segments.

## 4 NOISHHH-synthesized RNAV Trajectories

### 4.1 2D Optimization of RNAV Trajectories

The results presented in this Section relate to a situation where only the ***vertical*** flight path (profile) is optimized along a given horizontal flight path (route). In the considered example scenario, the horizontal flight path is defined by the existing RNAV approach to the "Polderbaan" (runway 18R) at Schiphol airport. Figure 3 illustrates the approach chart pertaining to this particular 18R RNAV approach, which is used during nighttime hours only.

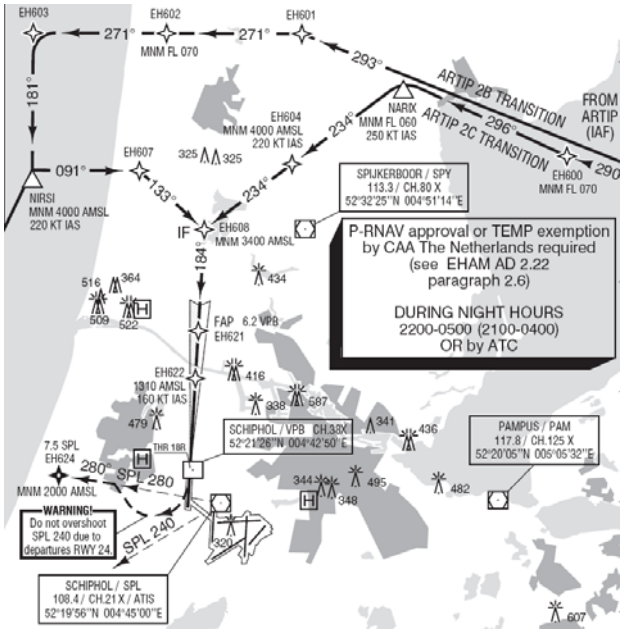


Fig. 3. Approach chart for the 18R RNAV approach at Schiphol airport [13].

The route considered leads the aircraft from NIRSI via waypoint EH608 to THR18R. The approach chart reveals that the route consists of three straight segments; however, in practice this means that an aircraft will connect the three straight segments using fly-by or fly-over turns. The glide slope phase starts at waypoint EH621.

The optimized vertical flight path needs to reflect all RNAV speed and altitude restrictions imposed along the way, while simultaneously honoring aircraft operating limits. At the initial route point, the specified speed is 220 kts IAS, while altitude is set at 4,000 ft. Due to the RNAV altitude constraint at waypoint EH608, the minimum altitude imposed at the start of the second turn is set at 3,400 ft. During the last straight segment before interception of the glide slope, flaps 5 is selected when IAS reaches 190 kts (the extension speed for the B737-300 at the considered gross weight). The IAS specified at the start of the glide slope phase is 170 kts. At the start of the glide slope phase, flaps 20 and gear down are selected. Finally, flaps 40 is selected when IAS reaches 140 kts at an altitude of at least 1,000 ft. The optimized trajectories are terminated at an altitude of 500 ft AGL. The part of the glide slope approach below 500 ft AGL, as well as the ground run during which the aircraft decelerates to a complete stop, have not been considered. If so desired, the noise contribution of these particular segments can be computed off-line and added to the overall noise impact. Since the influence of these final segments remains primarily limited to the (unpopulated) vicinity of the runway, these particular corrections have not been incorporated here.

To generate realistic flight paths several additional path/control constraints need to be imposed. First of all, bank angle is forced to remain within a range of 10 to 25 degrees during turns. In addition, altitude and IAS are not allowed to increase during the flight.

Table 1 summarizes the results obtained for the example scenario; it gives the values of fuel-consumed, expected number of awakenings and the transit time, optimized for three cases, viz., minimum number of expected awakenings, minimum fuel-consumed, and the maximum number of expected awakenings. The latter case serves to demonstrate the worst case bound for noise impact. In the maximum number of expected awakenings solution, both fuel flow

and transit time are higher than for the remaining two cases. This is primarily due to the fact that in the maximum number of expected awakenings solution the final segment is flown at low speed and at a relatively high thrust setting, especially above residential areas.

**Table 1. Comparison of optimal solutions obtained in the reference scenario.**

| case | fuel used (kg) | # awakenings | transit time (s) |
|---|---|---|---|
| minimum # awakenings | 151.0 | 535 | 338 |
| minimum fuel | 144.8 | 633 | 326 |
| maximum # awakenings | 170.8 | 822 | 356 |

## 4.2 3D Optimization of RNAV Trajectories

In this Section environmentally-optimized RNAV approach solutions are presented that have been obtained by a concurrent optimization of both ***lateral*** and ***vertical*** flight paths, using the RNAV-modified version of the NOISHHH tool.

To generate 3D-optimized RNAV trajectories using the RNAV-modified version of NOISHHH, the structure of the considered route needs to be a priori specified in terms of a sequence of RNAV segments. A meaningful structure can typically be identified from the 3D-optimized trajectory calculated using the original version of NOISHHH (i.e., without considering the RNAV requirements).

Figure 4 displays the 3D-optimized non-RNAV minimum-awakenings solution for the NIRSI approach to runway 18R at Schiphol airport. Based on the observed trajectory behavior, it is inferred that the corresponding RNAV minimum-awakenings route structure should consist of three straight (TF) segments with two radius-fixed (RF) turns in between, and ending with a 3° glide slope approach. The 3D-optimized minimum-awakenings RNAV solution based upon the assumed route structure is also shown in Figure 4. A close inspection of the results shows that the two solutions feature very similar ground tracks. Although the RNAV solution is principally based upon a route structure comprising 3 TF segments, the optimization process has reduced the middle TF segment to a limited proportion.

Figure 5 presents the time histories of altitude and speed for the two solutions. Since the RNAV solution is constrained to a constant flight path angle in each segment, the optimizer has less freedom to vary the altitude and speed profiles; this, combined with the small lateral flight path differences results in a slight increase in the expected number of awakenings of about 2.5%. This can be seen in Table 2, where the results for the two cases are summarized. The results include fuel consumption, expected number of awakenings and transit time.

**Table 2. Comparison of 3D-optimized RNAV and Non-RNAV minimum-awakenings solutions**

| case | fuel used (kg) | # awakenings | transit time (s) |
|---|---|---|---|
| Non-RNAV | 152.6 | 487 | 341 |
| RNAV | 152.2 | 499 | 342 |

Comparing the 3D optimization results with the 2D optimization results established in the reference scenario (see Table 1), shows that the 3D-optimized RNAV solution leads to a decrease in the number of awakenings of about 6.7% relative to the corresponding 2D-optimized RNAV solution. Figure 6 compares the current 18R RNAV route, as implemented in NOISHHH, with the horizontal flight path obtained in the 3D-optimized RNAV solution, shown earlier in Figure 4 (labeled optimal RNAV route). It can be observed that the main difference is the effectively wider turn of the optimal RNAV route. This wider turn particularly helps to alleviate the noise impact in the community of Castricum (located at coordinates (-8,26) in Figure 6). Furthermore, a slight difference in heading (about 3°) can be observed between the first segments of the two routes shown.

## 4.3 Parametric Study of 3D RNAV Solutions

A parametric study was conducted to assess the influence of various factors on the noise performance of the optimized RNAV trajectories. Notably, the influences of the

transit time, the RNAV route entry conditions, and the value of glide slope angle were investigated.

The transit time of a route is of particular importance in the context of time-based (4D) operations. Time-based operations have the potential of more tightly spaced final approach queues, without the need for controller intervention [14]. To investigate how much freedom an air traffic controller has in separating aircraft pairs, the minimum and maximum transit time for a given RNAV route were assessed. The route selected in this example corresponds to the 3D-optimized RNAV solution, presented in the previous Section (see Figure 6).

slope intercept. The minimum flight time for the RNAV route shown in Figure 6 is 225 seconds, while the maximum flight time is 247 seconds; this implies a small margin of only about 22 seconds. Implementation of a different flap speed schedule might improve this margin somewhat.

Several possibilities to further reduce the expected number of awakenings were explored. First of all, the location of the entry point and the initial track angle were optimized. Two other significant parameters that where varied (and optimized) relate to the glide slope angle ($\gamma_{gs}$) and the glide slope intercept altitude ($h_{gs}$) (note that currently the 3.0° glide path is intercepted at an altitude of 2,000 ft).

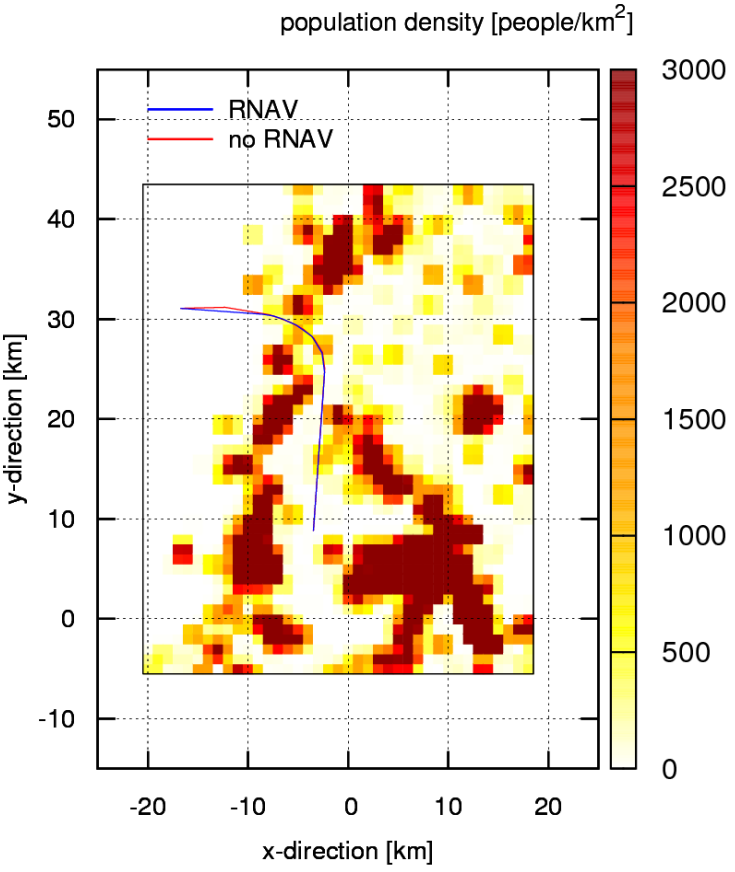


Fig. 4. Comparison of horizontal flight paths for RNAV and Non-RNAV minimum-awakenings approach solutions.

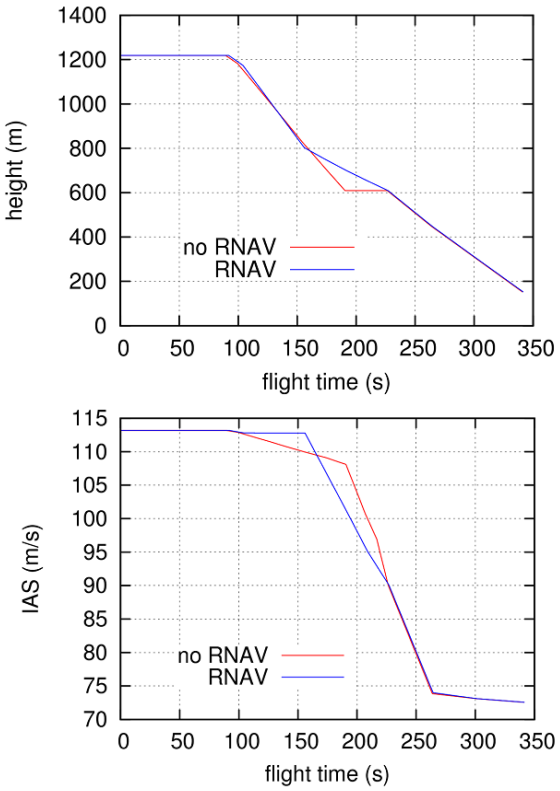


Fig. 5. Comparison of speed and altitude histories for RNAV and Non-RNAV minimum-awakenings approach solutions.

The flight times are calculated for the first part of the trajectory, just prior to glide

All cases are optimized with respect to the expected number of awakenings and Table 3

summarizes the results. The first entry in Table 3 relates to the reference solution, viz., the 3D awakenings-optimized RNAV solution obtained in the previous Section (see Table 2). The second entry shows the results for the case where the entry conditions where optimized. The remaining entries relate to the cases where the parameters glide slope intercept altitude and glide slope angle are optimized, either in isolation or in combination.

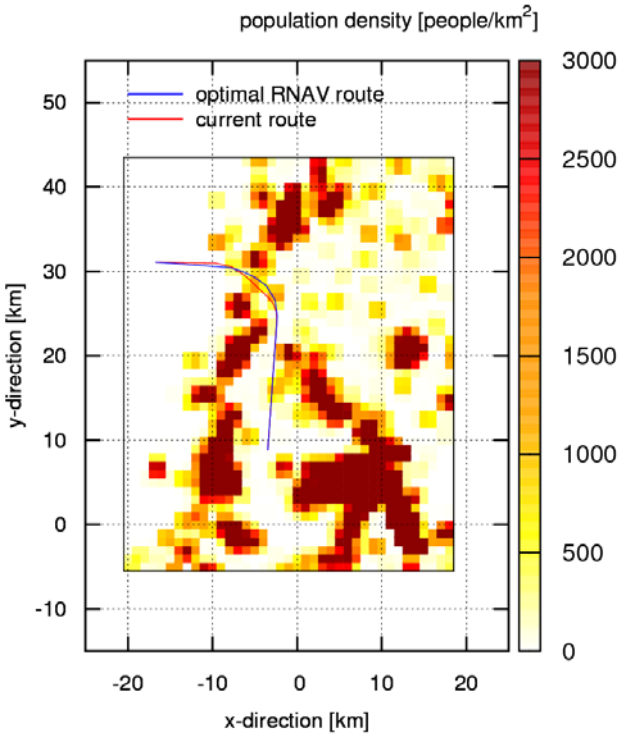


**Fig. 6. Comparison of 2D and 3D optimized RNAV trajectories (minimum awakenings criterion)**

Inspection of the results in Table 3 readily reveals that the influence of the various factors that have been examined remains surprisingly limited. Optimizing $h_{gs}$ and $\gamma_{gs}$ concurrently gives relatively the largest decrease in the expected number of awakenings (about 3%). For this case the value of $\gamma_{gs}$ is 2.2°, while $h_{gs}$ is 1427 ft. The optimal values reveal a shallow glide path which is intercepted at a relatively low altitude in comparison to the reference solution. Note that in the solution with optimized glide slope parameters, the distance to the runway threshold at the point of glide slope intercept is not significantly different from that of the reference solution (about 11.5 km). Since in both cases the glide slope is intercepted at the specified speed of 170 kts, this implies that actually more thrust is needed when flying along the 2.2° glide path in comparison to the 3.0° glide path approach. However, since the area underneath the glide path is largely uninhabited, the awakenings performance is hardly influenced by the added thrust. The true benefit enjoyed by the solution with optimized glide slope parameters results from the part of the trajectory preceding glide slope intercept. Indeed, a lower interception altitude implies that less power needs to be added along the way. Since the part of the trajectory preceding glide slope intercept does overfly areas that are inhabited, the affected residential communities will directly benefit from reduced thrust levels. It should be noted that it is conceivable that the observed trajectory behavior is a direct consequence of the fact that speed has been specified at glide slope intercept. This needs to be investigated in future research.

**Table 3. Performance benefits resulting form various potential noise mitigation options**

| Case | fuel used (kg) | Awakenings | transit time (s) |
|---|---|---|---|
| reference case | 156.2 | 499 | 342 |
| free initial point | 153.8 | 499 | 342 |
| free $h_{0gs}$ | 143.0 | 489 | 334 |
| free $\gamma_{gs}$ | 156.8 | 498 | 344 |
| free $h_{0gs}$ and $\gamma_{gs}$ | 154.5 | 482 | 339 |

## 5 Conclusions

Through the course of this research, we have developed a novel tool for synthesizing environmentally-optimized RNAV approach trajectories. This new development is based on an extension of a tool called NOISHHH which was developed earlier for the analysis and design of noise abatement procedures around airports.

Although the results presented herein remain restricted to noise optimization only, the RNAV-extension tool also shows promise for generating trajectories optimized with respect to emission of gaseous pollutants.

In the numerical examples it was demonstrated that introducing RNAV navigation requirements in the trajectory optimization formulation results, as expected, in a slight decrease in environmental performance. A more significant result is that the RNAV routes that were environmentally-optimized using NOISHHH proved to offer a substantial improvement in environmental performance over existing RNAV routes.

The next step in designing routes with NOISHHH will be the use of other aircraft models to generate routes that are suitable for a larger number of aircraft types. Furthermore, the design of RNAV departure routes, optimized with respect to noise or emissions, will be pursued in a follow-on study.

## References

[1] Visser, H.G., Hebly S.J. and Wijnen R.A.A., Improving the Management of the Environmental Impact of Airport Operations. In: *New Transportation Research Progress*, ISBN: 978-1-60456-032-9, Nova Science Publishers, 2008, pp. 1-65.

[2] Erkelens, L.J.J. Research into New Noise Abatement Procedures for the 21st Century, *Proc. of the AIAA Guidance, Navigation, and Control Conference*, Denver CO, U.S.A., AIAA-2000-4474, August 2000.

[3] De Gaay Fortman, Van Paassen, M.M., Mulder, M., In 't Veld, A.C. and Clarke, J.-P., Implementing Time-Based Spacing for Decelerating Approaches. *Journal of Aircraft*, Vol. 44, No.1, 2007, pp.106-118

[4] Prats, X., Nejjari, F., Puig, V., Quevedo, J. and Mora-Camino, F. A framework for RNAV trajectory generation, *Proc. of the 2nd Congress on Research in Air Transportation,* Belgrade, Serbia, 2006.

[5] Visser, H.G. and Wijnen, R.A.A. Optimization of Noise Abatement Departure Trajectories. *Journal of Aircraft,* Vol. 38, No. 4, 2001, pp. 620-627.

[6] Wijnen, R.A.A. and Visser, H.G., Optimal Departure Trajectories with Respect to Sleep Disturbance. *Aerospace Science and Technology*, Vol. 7, January 2003, pp. 81-91.

[7] Visser, H.G. and Wijnen, R.A.A., Optimisation of Noise Abatement Arrival Trajectories. *The Aeronautical Journal*, Vol. 107(1076), 2003, pp.607-615.

[8] Visser, H.G., Generic and Site-Specific Criteria in the Optimization of Noise Abatement Trajectories. Transportation Research Part D: Transport and Environment, Vol. 10, No. 5, 2005, pp.405-419.

[9] International Civil Aviation Organization, *ICAO Engine Exhaust Emissions Data Bank*. ICAO Doc. 9646, 1st Edition, 1995.

[10] Federal Interagency Committee on Aviation Noise (FICAN). *Sleep Disturbance caused by Aviation Noise*. U.S.A., March 1997.

[11] Office of Environment and Energy, *Integrated Noise Model (INM) Version 6.0 Technical Manual*. Rept. FAA-AEE-02-01, 2002.

[12] Sprong, K.R. Haltli, B.M., DeArmon, J.S. and Bradley, S. Improving Flight Efficiency through Terminal Area RNAV. *Proc. Of the 6th USA-Europe ATM Seminar*, Baltimore, U.SA, paper No. 7, 2005.

[13] http://www.ais-netherlands.nl/

[14] Ruigrok, R. and Korn, B. Combining 4D and ASAS for Efficient TMA Operations. *Proc. of the AIAA Aviation Technology, Integration and Operations Conference,* Belfast, Northern Ireland, AIAA 2007-7745, September 2007.

## Copyright Statement